

**DAMAGE STRUCTURE OF AUSTENITIC STAINLESS STEEL 316LN IRRADIATED AT LOW TEMPERATURE IN HFIR** - N. Hashimoto (Oak Ridge National Laboratory), E. Wakai (Japan Atomic Energy Research Institute), J. P. Robertson (ORNL), M. L. Grossbeck (ORNL), and A. F. Rowcliffe (ORNL)

## OBJECTIVE

The purpose of this work is to investigate the microstructure of austenitic stainless steel 316LN irradiated at low temperatures and to damage levels of about 3 dpa and to relate the microstructure to mechanical behavior.

## SUMMARY

TEM disk specimens of austenitic stainless steel 316LN irradiated to damage levels of about 3 dpa at irradiation temperatures of either about 90 °C or 250 °C have been investigated by using transmission electron microscopy. The irradiation at 90 °C and 250 °C induced a dislocation loop density of  $3.5 \times 10^{22} \text{ m}^{-3}$  and  $6.5 \times 10^{22} \text{ m}^{-3}$ , a black dot density of  $2.2 \times 10^{23} \text{ m}^{-3}$  and  $1.6 \times 10^{23} \text{ m}^{-3}$ , respectively, in the steels, and a high density ( $< 1 \times 10^{22} \text{ m}^{-3}$ ) of precipitates in matrix. Cavities could be observed in the specimens after the irradiation. It is suggested that the dislocation loops, the black dots, and the precipitates cause irradiation hardening, an increase in the yield strength and a decrease in the uniform elongation, in the 316LN steel irradiated at low temperature.

## PROGRESS AND STATUS

### 1. Introduction

An austenitic stainless steel, 316LN-1G is the structural first wall and shield material for the International Thermonuclear Experimental Reactor (ITER) [1]. The proposed operational temperature range for the structure is from 100 °C to 250 °C, which is below the temperature regimes for void swelling and for grain boundary embrittlement. For austenitic stainless steels, neutron irradiation at low temperature increases the yield strength and decreases the uniform elongation, and fracture toughness. As reported earlier, the magnitudes of these changes are both temperature and dose dependent [2-3].

The objective of this study is to investigate microstructure of 316LN austenitic stainless steel irradiated at low temperatures up to 3 dpa in order to relate the microstructure to the changes in mechanical properties.

### 2. Experimental Procedure

The chemical composition of the 316LN used in this study falls within the specifications for the ITER reference grade (316LN-1G) as shown in Table 1. Standard 3-mm diameter transmission electron microscopy (TEM) disks were punched from 0.25-mm thick sheet stock, and then these disks were solution annealed. The disks were irradiated in the HFIR in the capsules of HFIR-MFE-JP-17 and -JP-18 to neutron fluences producing 3 dpa. These capsules were designed for irradiation temperatures of either 90 °C (capsule HFIR-MFE-JP18) or 250 °C (HFIR-MFE-JP-17) [4-6]. The helium concentration generated as a result of transmutation of nickel was about 65 appm; this is in the range expected for the ITER first wall blanket and shield structure after a neutron exposure of 3 dpa.

TEM specimens were thinned using an automatic Tenupol electropolishing unit in a shielded glove box. TEM disks were examined using a JEM-2000FX (LaB<sub>6</sub>) transmission electron microscope. The foil thickness were measured by thickness fringes in order to quantify defect density values.

Table 1. Chemical compositions of 316LN (wt%)

Steel	Fe	Cr	Ni	Mo	Mn	Si	C	N
316LN	Bal.	17.4	12.3	2.3	1.8	0.46	0.024	0.06
316LN-1G	Bal.	17.0	12.0	2.3	1.6	0.50	0.015	0.06
		18.0	12.5	2.7	2.0		0.030	0.08

### 3. Results

#### 3.1 Dislocations and dislocation loops

Fig. 1 shows dislocations or dislocation loops in 316LN before and after irradiation up to 3 dpa. The electron micrographs were taken with beam direction **B** close to  $\langle 110 \rangle$ . Fig. 1(a) is a bright-field image in the unirradiated specimen, and Figs. 1(b) and 1(c) are dark-field images in the specimens irradiated at 90 °C and 250 °C, which are taken using a streak in the diffraction pattern arising from the faulted loops. The loops observed in specimens irradiated at 90 °C or 250 °C were Frank type faulted loops on  $\{111\}$  planes, which were identified by the weak beam dark-field image. The irradiation at 250 °C induced a slightly higher dislocation loop density of  $6.5 \times 10^{22} \text{ m}^{-3}$  with a slightly smaller mean diameter of 7.0 nm compared with the irradiation at 90 °C. The total dislocation density, which means the total line length of loops per an unit volume, after irradiation at 250 °C is  $1.4 \times 10^{15} \text{ m}^{-3}$ , which is about twice as high as the loop density observed after the 90 °C irradiation. The irradiation also induced small defect clusters (black dots) in the matrix.

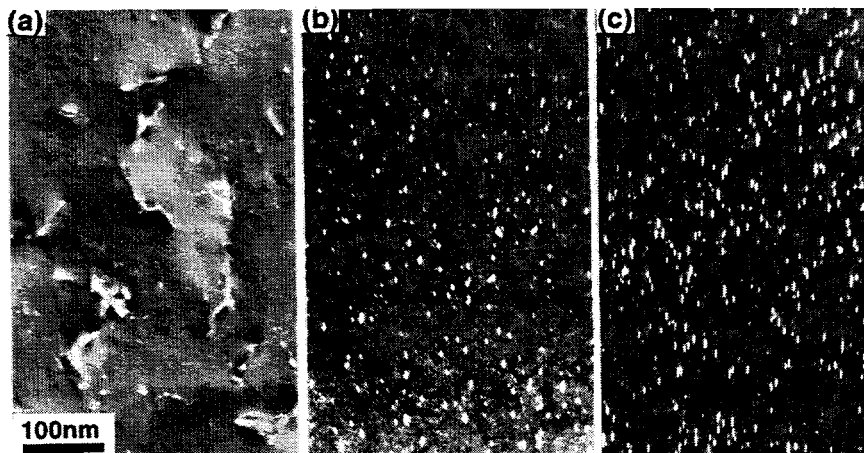


Fig. 1. Dislocations or dislocation loops in 316LN before and after HFIR irradiation up to 3 dpa. Micrographs were taken with beam direction **B** close to  $\langle 110 \rangle$ . (a) is a bright-field image in the unirradiated specimen, and (b) and (c) are dark-field images taken using a streak arising from faulted loops in the specimens irradiated at 90 °C and 250 °C

Fig. 2 shows the black dot defect in 316LN after irradiation up to 3 dpa. The number density and the mean diameter of black dots at 90 °C and 250 °C were  $2.2 \times 10^{23} \text{ m}^{-3}$  and 2 nm, and  $1.6 \times 10^{22} \text{ m}^{-3}$  and 2 nm, respectively. In the present work, the black dot density and the mean diameter were measured in relatively thick foils ( $t < 100 \text{ nm}$ ). The actual black dot number density and mean diameter may be somewhat higher and lower, respectively. The dislocation density in the unirradiated specimen and the dislocation loop density and the black dot density of the irradiated specimens are shown in Table 2.

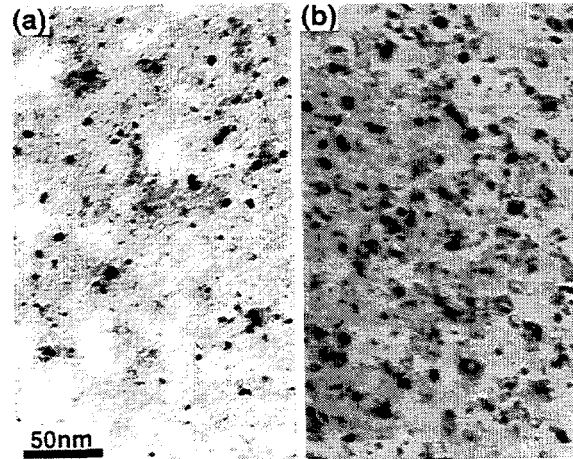


Fig. 2. The black dot in 316LN after HFIR irradiation up to 3 dpa. (a) and (b) are bright-field images in the specimens irradiated at 90 °C and 250 °C. The average thickness is about 100 nm.

Table 2. Summary of dislocation, dislocation loop, and black dot density of 316LN irradiated to 3 dpa. The average thickness of measured area is 100 nm.

Condition	Black Dot		Dislocation or dislocation loop		
	Number density ( $\text{m}^{-3}$ )	Mean diameter (nm)	Number density ( $\text{m}^{-3}$ )	Mean diameter (nm)	Total dislocation density ( $\text{m}^{-2}$ )
Before irradiation	-	-	-	-	$1 \times 10^{14}$
Irr. at 90 °C	$2.2 \times 10^{23}$	2	$3.5 \times 10^{22}$	7.6	$8.3 \times 10^{14}$
Irr. at 250 °C	$1.6 \times 10^{23}$	2	$6.5 \times 10^{22}$	7.0	$1.4 \times 10^{15}$

Fig. 3 shows another dark-field image in the specimen irradiated at 250 °C, which was obtained from a streak observed in the diffraction pattern. The defects were dislocation loops on {110} planes. The loops on {110} planes were observed only in the specimen irradiated at 250 °C. The number densities and the mean diameter of the loops is  $1.2 \times 10^{21} \text{ m}^{-3}$  and 10.2 nm, respectively.

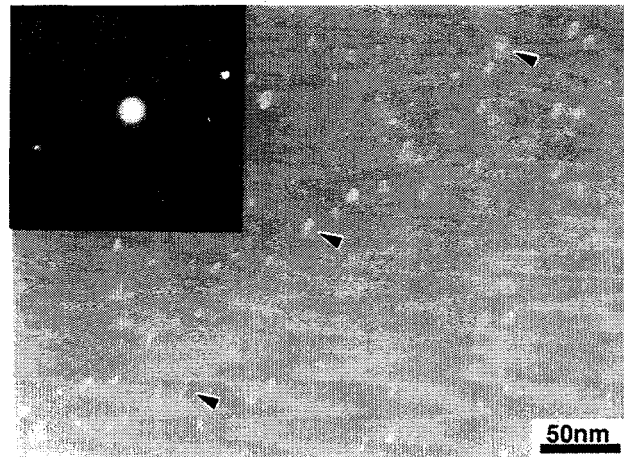


Fig. 3. Dark-field image formed using a streak observed in the diffraction pattern in the specimen irradiated at 250 °C in HFIR. Loops on {110} are observed.

### 3.2 Precipitate evolution

Fig. 4 shows the microstructures of 316LN before and after irradiation up to 3 dpa. As seen in Fig. 4, the annealed 316LN had no precipitate. The irradiation at both 90 °C and 250 °C induced precipitates, which could be identified as G phase from a spacing of the moiré fringe and the diffraction pattern. The number density and the mean diameter of G formed at 90 °C and 250 °C are  $2.0 \times 10^{22} \text{ m}^{-3}$  and 5 nm, and  $2.0 \times 10^{22} \text{ m}^{-3}$  and 7 nm, respectively.

As shown in Fig. 5, the irradiation at 90 °C and 250 °C also induced M<sub>23</sub>C<sub>6</sub> carbide in the matrix but not on grain boundaries; these were identified from the spacing of the moiré fringe. The number density and the mean diameter of M<sub>23</sub>C<sub>6</sub> at 90 °C and 250 °C are nearly equal, and the values are about  $<1 \times 10^{19} \text{ m}^{-3}$  and 14 nm, respectively. There is no clear difference in the precipitate densities between irradiation temperatures. The precipitates observed in the specimens are summarized in Table 3.

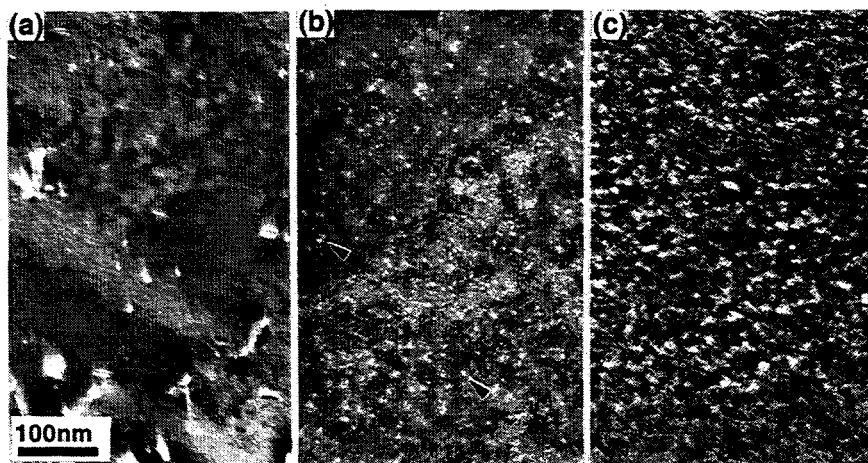


Fig. 4. Microstructure of 316LN before and after irradiation up to 3 dpa. (a) is a dark-field image in the unirradiated specimen, and (b) and (c) are dark-field images in the specimens irradiated at 90 °C and 250 °C. Precipitates are observed with moiré fringes in the specimens irradiated at 90 °C and 250 °C.

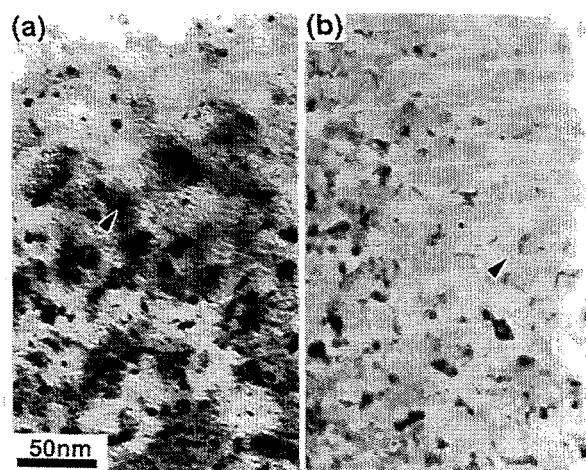


Fig. 5.  $M_{23}C_6$  carbide in 316LN after HFIR irradiation up to 3 dpa. (a) and (b) are bright-field images in the specimens irradiated at 90 °C and 250 °C.

Table 3. Precipitate statistics before and after irradiation at 90 and 250 °C up to 3 dpa

Steel	ppt.	Before irradiation		After irradiation (90 °C)		After irradiation (250 °C)	
		Mean diameter (nm)	Number density ( $m^{-3}$ )	Mean diameter (nm)	Number density ( $m^{-3}$ )	Mean diameter (nm)	Number density ( $m^{-3}$ )
316LN	$M_{23}C_6$	-	-	13	$<1 \times 10^{19}$	14	$<1 \times 10^{19}$
	G	-	-	5	$2 \times 10^{22}$	7	$2 \times 10^{22}$

#### 4. Discussion

##### 4.1 Microstructures

HFIR irradiation up to 3 dpa induced the dislocation loop density of about  $5 \times 10^{22} m^{-3}$  with mean diameter of 7 nm, as given in Table 2. The dislocation loops formed under irradiation both at 90 °C and 250 °C have been identified as Frank type faulted loops, which are lying on  $\{111\}$  planes with Burgers vectors of type  $b = (1/3)a_0 \langle 111 \rangle$ . The dislocation loop density at 90 °C is slightly higher than that at 250 °C. Previous studies have shown that the both the nature and number density of defects formed in type 316 austenitic stainless steel during neutron irradiation is strongly dependent on irradiation temperature [7-9], Zinkle et. al [7] characterize a low temperature regime as extending from the onset of vacancy motion (annealing Stage 3) up to the temperature where vacancy clusters created in the displacement cascade become thermally unstable (annealing Stage 5). The current study is within this low temperature regime. The number densities of faulted Frank loops reported here are consistent with the values of  $5 \times 10^{22} m^{-3}$  reported by Maziasz for irradiation at 60 °C and by Tanaka for irradiation at 300 °C.

At these low temperatures, the total dislocation density is dominated by faulted loops [10,11], and the total dislocation densities were calculated from the dislocation loop density and the mean diameter as  $8.3 \times 10^{14} m^{-2}$  and  $1.4 \times 10^{15} m^{-2}$  at 90 °C and 250 °C, respectively. These values are consistent with the results of previous analysis of austenitic stainless steels irradiated in HFIR [12].

At higher irradiation temperatures ( $> 450$  °C), Frank loops tend to unfault to form the lower-energy perfect loop configuration with  $b = (1/2)a_0\langle 110 \rangle$  Burgers vectors, which can glide to interact and form network dislocations [7]. In this experiment, however, dislocation loops on {110} planes with mean size of  $> 10$  nm were observed following irradiation at 250 °C. It seems that there is sufficient mobility at 250 °C for the unfauling reaction, which is triggered by physical impingement of adjoining Frank loops as a result of loop growth [13], to occur for ~2% the Frank loop populations.

The irradiation also induced small defect clusters (black dots) in the matrix. The visibility of very small clusters depend on the foil thickness, the visible cluster density in very thin foils was higher than that found in thick foils [14]. In the present work, the black dot density and the mean diameter were measured in relatively thick foils ( $t \sim 80$  nm). Therefore, the actual black dot number density and mean diameter may be somewhat higher and lower, respectively.

In general, there has been no evidence of fine precipitation in 316 type stainless steels after neutron irradiations at 55-250 °C at doses of  $> 1-2$  dpa [14,15]. The HFIR irradiation at 90 °C and 250 °C, however, induced precipitates, identified as G phase and M<sub>23</sub>C<sub>6</sub> from a spacing of the moiré fringe and/or diffraction pattern, in the matrix and not on grain boundaries. G phase is a radiation-induced precipitate, according to ref.15, traces of G phase were also found in JPCA irradiated in HFIR at 300 °C. On the other hand, M<sub>23</sub>C<sub>6</sub> is a radiation-enhanced thermal phase, and is produced more abundantly at lower temperatures during neutron irradiation [16].

#### 4.2 Relation between microstructures and mechanical properties

Load elongation curves for SS-3 tensile specimens of 316LN irradiated and tested at 90 °C and 250 °C are shown in Fig. 6 and the corresponding tensile data are shown in Table 4 [17]. The radiation-induced changes in tensile properties are more severe at 250 °C than at 90 °C.

Table 4. Tensile properties of solution annealed 316LN

Dose dpa	Irr.Temp. °C	Test Temp. °C	YS MPa	UTS MPa	Eu %	Et %
0	-	25	298	582	62.0	68.5
0	-	90	285	516	50.2	57.2
0	-	250	214	451	40.8	51.3
2.9	83-101	90	610	674	37.7	45.0
2.9	83-101	90	605	677	37.0	46.1
3.0	250-300	250	760	764	11.7	18.8
3.0	250-300	250	724	735	12.7	20.8

Irradiation at 90 °C increased the yield strength from 285 MPa up to 600 MPa, and resulted in a modest reduction in both the strain hardening rate and the uniform elongation. A larger increase in yield strength occurred for the irradiation at 250 °C. Following an initial yield drop, uniform strain exceeded 10 % in spite of a very low rate of strain hardening. These data are plotted in Fig. 6(a) and the corresponding number density data for dislocation loops, black dots and precipitates are shown in Fig. 6(b). While the density of precipitates is nearly constant, the density of dislocation loops and black dots increase and decrease respectively with irradiation temperature.

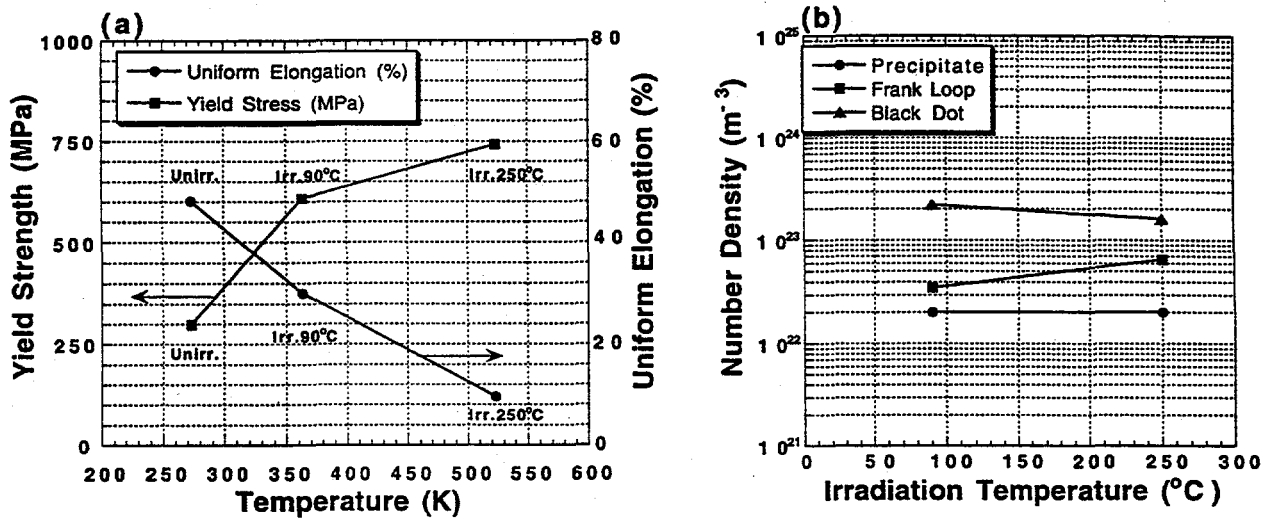


Fig. 6. Dependence of irradiation temperature on the dislocation loop density, the black dot density and the precipitate density; (a), and the yield strength and the uniform elongation; (b).

According to the theory of hardening [18,19], the yield stress change due to dislocation loops,  $\Delta\sigma_y$ , is expressed the following equation:

$$\Delta\sigma_y = M\alpha\mu b(Nd)^{1/2},$$

where  $M$ ,  $\alpha$ ,  $\mu$ ,  $b$ ,  $N$  and  $d$  are the Taylor factor [18], barrier strength of obstacles, shear modulus, Burger's vector, density of dislocation loops and mean diameter of dislocation loops, respectively. The contributions of the Frank loops and black dots are as follows:

$$(\Delta\sigma_y)^{1/2} = (\Delta\sigma_{\text{Frank Loop}})^{1/2} + (\Delta\sigma_{\text{Black Dot}})^{1/2},$$

With the Taylor factor of 3.06 [20], the shear modulus of  $58 \times 10^3$  MPa and the value of  $\alpha_{\text{Black Dot}} = 0.146$  [21], a value of  $\alpha_{\text{Frank Loop}} = 0.47$  and  $0.55$  are obtained at  $90^\circ\text{C}$  and at  $250^\circ\text{C}$ , respectively. These values of  $\alpha = 0.47$  and  $0.55$ , which are obtained in the present work, are in good agreement with the data of Odette and Frey [22] and of Gamer et al. [23]. Further measurements of the defect densities are in progress using thinner regions of the foil to improve visibility. Although the number densities of defect clusters and Frank loops change only slightly between  $90^\circ\text{C}$  and  $250^\circ\text{C}$ , there is significantly less strain hardening capacity at the higher temperature. This suggests that there is a tendency for dislocation channeling to occur at  $250^\circ\text{C}$  and for deformation to be more homogeneous at  $90^\circ\text{C}$ . Further analysis of these phenomenon is in progress.

## ACKNOWLEDGMENTS

This research was supported in part by an appointment to the Oak Ridge National Laboratory Postdoctoral Research Associates Program administered jointly by the Oak Ridge Institute for Science and Education and Oak Ridge National Laboratory.

## REFERENCES

1. A.F. Rowcliffe, "ITER Material Assessment Report for Stainless Steels", ITER Doc. G A1 DDD 1 97-12-08 W 0.2, December, 1997.
2. J.E. Pawel, A.F. Rowcliffe, D.J. Alexander, M.L. Grossbeck, and K. Shiba, *J. Nucl. Mater.*, **233-237** (1996) 202-206
3. D.J. Alexander, J.E. Pawel, M.L. Grossbeck, A.F. Rowcliffe, and K. Shiba, "Fracture Toughness of Irradiated Candidate Materials for ITER First Wall/Blanket Structures: Summary Report", *Fusion Reactor Materials Semiannual Report for Period Ending December 31, 1995*, DOE/ER-0313/19, 1996, p. 204.
4. A.W. Longest, D.W. Heatherly, K.R. Thomas, and J.E. Corum, "Design and Fabrication of HFIR-MFE-JP Target Irradiation Capsules," *Fusion Reactor Materials Semiannual Report for Period Ending March 31, 1991*, DOE/ER-0313/10, 1991, p. 3.
5. A.W. Longest, D.W. Heatherly, J.E. Wolfer, K.R. Thomas, and J.E. Corum, "Fabrication and Irradiation of HFIR-MFE-JP-17, -18, and -19 Target Irradiation Capsules," *Fusion Reactor Materials Semiannual Report for Period Ending September 30, 1991*, DOE/ER-0313/11, 1992, p. 30.
6. A.W. Longest, D.W. Heatherly, K.R. Thomas, and J.E. Corum, "Fabrication and Irradiation of HFIR-MFE-JP Target Irradiation Capsules," *Fusion Reactor Materials Semiannual Report for Period Ending March 31, 1992*, DOE/ER-0313/12, 1992, p. 24.
7. S.J. Zinkle, P.J. Maziasz and R.E. Stoller, *J. Nucl. Mater.*, **206** (1993) 266
8. M. Kiritani, *Ultramicroscopy*, **39** (1991) 135-159.
9. P.J. Maziasz and C.J. McHargue, *Int. Mater. Rev.*, **32** (1992) 190.
10. H.R. Brager and J.L. Straalsund, *J. Nucl. Mater.*, **46** (1973) 134.
11. P.J. Barton, B.L. Eyre and D.A. Stow, *J. Nucl. Mater.*, **67** (1977) 181.
12. P.J. Maziasz, Effect of He Content on Microstructural Development in Type 316 Stainless Steel under Neutron Irradiation, ORNL-6121, Oak Ridge, TN (1985)
13. P.J. Maziasz and C.J. McHargue, *Int. Mater. Rev.*, **32** (1987) 190.
14. S.J. Zinkle, *J. Nucl. Mater.*, **150** (1987) 140-158.
15. P.J. Maziasz, *Am. Nucl. Soc. Trans.*, **39** (1981) 433.
16. P.J. Maziasz, *J. Nucl. Mater.*, **169** (1989) 95.
17. Brager, F.A. Garner, F.R. Gilbert, J.E. Flinn and W.G. Wolfer, in : *Radiation Effects in Breeder Reactor Structural Materials*, eds. M.L. Bleiberg and J.W. Bennet (TMS-AIME, New York, 1977) p. 727.
18. U.F. Kocks, *Metall. Trans.*, **1** (1970) 1121.
19. P.M. Kelly, *International Metallurgical Reviews*, Vol.18 (1973) 31
20. H.R. Higgy and F.H. Hammad, *J. Nucl. Mater.*, **55** (1975) 177.
21. R.L. Sindelar, "Reactor Materials Program - Microstructural and Mechanical Response of Types 304, 304L, and 308 Stainless Steels to low temperature Neutron Irradiation (U)", **WSRC-TR-93-196**, June (1993)
22. G.R. Odette and G. Frey, *J. Nucl. Mater.*, **85-86** (1979) 817
23. F.A. Garner, M. Hamilton, N. Panayotou, G. Johnson, *J. Nucl. Mater.*, **103-104** (1981) 803